



Disk structures and the handiwork of triaxial tumbling dark halos

D. Chakrabarty¹ and J. Dubinski²

¹ School of Physics and Astronomy, University of Nottingham, Nottingham, UK
e-mail: dalia.chakrabarty@nottingham.ac.uk

² Department of Astronomy and Astrophysics, University of Toronto, Toronto, ON, Canada

Abstract. The triaxial and tumbling nature of dark matter halos has been established through cosmological simulations. Such a configuration can then potentially impart a slowly changing torque on the galactic disk from outside. We use this idea as the motivation to seek the possible dynamical effects of such a halo in terms of the development of disk structures. To check this effect, we perform a series of N-body simulations and some analytical calculations, in which we study the disk configuration, as affected by an imposed, slowly tumbling, external quadrupole. For our simulations, the amplitude of this quadrupole is gauged from a sample of halos that we establish through cosmological, N-body simulations. When used as an input, such a quadrupole is found to generate pronounced spirality, long-lived warps and fast bars in model galactic disks that are inherently stable against such instabilities for a long time. Our analytical calculations are found to indicate similar trends in disk stellar motion, as noted in our simulations.

Key words. dark matter – galaxies: structure – methods: N-body simulations

1. Introduction

The making of sustained galactic warps is an issue that is still not satisfyingly answered – this in spite of focused work over the years (Binney 2007). Basically, for the outer parts of the disk to warp, the halo needs to manifest asymmetries. Workers in the field have attempted to seek the source of such asymmetries. Broadly speaking, the same has been attributed to

- tidal torques from disk-halo misalignment (Toomre 1983; Sparke & Casertano 1988; Kuijken 1991; Nelson & Tremaine 1995; Binney et al. 1998)

- gas infall (Jiang & Binney 1999; Shen & Sellwood 2006; van der Kruit 2007)
- tidal fields of companions - warp in M31 from one or both companions (Kalirai et al. 2006); Large Magellanic Cloud (LMC) triggered warp in the Milky Way (MW, Weinberg 1998; García-Ruiz et al. 2002; Weinberg & Blitz 2006).

The idea that the disk warps when torqued by a misaligned halo, is appealing, given that this idea offers an internal mechanism for explaining warps. Such disk-halo misalignment is expected to result in the precession of nearly circular orbits. However, a major flaw in this argument stems from the work by Dubinski & Kuijken (1995), who demonstrated that the

precessing disk will align with the inner halo within a few dynamical times, owing to dynamical friction; in fact, the coupling between the inner halo and the disk was shown to be tight. This motivates us to seek an alternative solution to the problem of triggering and sustaining warps. One answer could be to seek disk-halo misalignment at radii that exceed the extent of gravitational influence of the disk.

In this work, we pursue this line of argument and examine the handiwork of the outer halo on the generation of disk structures, such as not only the warp, but also the bar and spiral-ity. The outer dark halo is treated as triaxial and slowly tumbling. Thus, the disk stays tightly coupled with the inner halo (as in Bailin et al. 2005) but is affected by the tidal field of the outer halo. Dark halos realised in Λ CDM simulations have been noted to be typically flattened (Barnes & Efstathiou 1987; Frenk et al. 1988; Dubinski & Carlberg 1991; Warren et al. 1992; Jing & Suto 2002). This triaxiality can be responsible for various dynamical effects that get imprinted on disks, such as oval distortions, warps and bars (Sparke 1984; Franx & de Zeeuw 1992; Sackett et al. 1994; Kuijken & Tremaine 1994; Weinberg 1998; Sellwood 2003; Berentzen et al. 2006). The tumbling nature of dark halos is also brought out in simulations performed with the Λ CDM cosmology (Dubinski 1992; Bureau et al. 1999; Bailin & Steinmetz 2004). In fact, Bailin & Steinmetz (2004) report that the distribution of halo tumbling speeds is log-normal in form, with a mean at $\Omega_p = 0.15 \text{ km s}^{-1} \text{ kpc}^{-1}$, which is the same as a tumbling period of about 44 Gyr. It is the effect of such triaxial and tumbling dark halos that we report here.

In order for us to probe the same, the first thing we will need to constrain is the strength of the tidal field of the outer halo. This is discussed in Sect. 2. We mention the framework of our simulations in Sect. 3 and report our results in Sect. 4. We wind up the paper with a discussion of the comparison between our numerical results and analytical calculations.

2. Amplitudes of the tidal field of halos on disks

We compute the expected ranges of the amplitude of the quadrupolar term in the potential of the dark halo, from cosmological N-body simulations. As mentioned above, the tidal torquing from the halo is expected to have an effect on the disk only at radii that are beyond the gravitational influence of the disk, which is approximately set by the disk extent. Thus, if the galaxy is modelled with an NFW dark halo (Navarro et al. 1995), then the scale radius r_s could be considered to be a fairly representative indicator of the disk extent. Thus, we are required to calculate the strength of the quadrupolar term only for radius $r > r_s$. In fact, we perform yet another set of calculations even further out, for $r > 2r_s$.

Our simulations are performed with the GOTMP code (Dubinski 1996), using 512^3 particles in a cube of dimension $L = 70 h^{-1} \text{ Mpc}$ and was run from a redshift of 70, in 2800 equal time steps. We used $\Omega_\Lambda = 0.7$, $\Omega_m = 0.3$, $\sigma_8 = 0.9$ and $h = 0.7$ (Spergel et al. 2007). Halos were extracted using the following method.

- First we identify the centres of our candidate halos using a friends-of-friends algorithm.
- We identify halos from our sample of candidate halos by monitoring particles in a spherical region around the identified centres, to $r = r_{200}$ and fit NFW profiles to these particles sets.
- Only those sets that admit a fit to a χ^2 value in excess of a pre-set threshold, are accepted as halos.

This procedure offers us a sample of about 2200 undisturbed halos. The recorded particle distribution for each of these halos is used to obtain the amplitude of the quadrupolar term in the halo potentials. This is obtained via multipole expansion, only at radii in excess of r_s (in the first stage) and $2r_s$ (in the second). Now, the halo potential at all $r < r_0$ can be expanded in terms of spherical harmonic functions, the l, m^{th} coefficient of which is the term c_{lm} (say). Then c_{lm} can be expressed as sum of the con-

tributions from all the particles at $r > r_0$ in the halo at hand, in terms of the usual spherical (r, ϕ, θ) coordinates that represent particle location. So we compute c_{lm} for $r_0 = r_s$ and $2r_s$. Thus, a ready measure of the strength of the l^{th} term in the external potential of a halo is

$$c_l = \left(\sum_{m=-l}^{m=l} \frac{|c_{lm}|^2}{2l+1} \right)^{1/2} \quad (1)$$

where we are interested in the quadrupolar term only, i.e., in c_2 . It is this c_2 parameter that we compute from each of our recorded halo particle distributions. Given that this strength parameter c_2 will depend on halo properties (mass), we renormalise the sample halos to have the same scale mass and scale radius. In fact, we scale all our model halos to a putative Milky Way model and refer to the resulting normalised c_2 parameter as $c_{2,\text{MW}}$.

Now, one direct way of gauging the strength of a halo quadrupolar term is by comparing this normalised quadrupolar amplitude of the halo at hand, to the strength of the tidal field of an LMC-type satellite felt by the Galactic disk (= $c_{2,\text{LMC}}$, say). Thus, if for a given halo, the ratio $q_{\text{tidal}} = c_{2,\text{MW}}/c_{2,\text{LMC}}$ is about 1, then it implies that the effect of the tidal field of the halo is nearly the same as that of the LMC on the Galactic disk, which is not too potent. Hence if $q_{\text{tidal}} \approx 1 \implies$, the halo is rather weak - as weak as the LMC on the Galactic disk. We calculate q_{tidal} for the whole sample of recorded halos, for $r_0 = r_s$ and $r_0 = 2r_s$. For the former r_0 value, the recovered q_{tidal} has a mean at about 25, while for $r_0 = 2r_s$, it is distributed around a value of about 5. Thus, the strength of the external quadrupole of the outer triaxial halo is between 5 and 25 times the strength of the LMC tidal field.

3. Simulations

We carry out N-body simulations of model galaxies that are perturbed by an external quadrupole that is tumbling at a pattern speed of Ω_p . The code used in these simulations is modified from the parallelised treecode used by Dubinski (1996), to include the quadrupole. For all particles at a radius $r > r_0$, the field

due to the external potential is shut off. We use $r_0 = 60$ kpc. The model galaxies are represented by a disk with a central bulge and a halo; these are the MW and M31 models given by Widrow & Dubinski (2005). These models are characterised by a Hernquist bulge, an exponential disk and an NFW halo. The MW model is slightly bar unstable while the M31 model was shown to be robust to bar formation till 10 Gyr. Our best runs are done with 1.5 million particles to describe the disk, 0.5 million for the bulge and 2 million for the halo.

The quadrupole strength used in the runs implies a q_{tidal} of about 6. This quadrupole is also made to rotate at tumbling rates of $\Omega_p = 0.11, 0.22, 0.44$, and $0.88 \text{ km s}^{-1} \text{ kpc}^{-1}$ corresponding to tumbling periods of $T = 56, 28, 14$, and 7 Gyr respectively. The misalignment with the disk is imposed through a tilt of 30° between the disk and the quadrupole.

We use 800 timesteps in intervals of 0.55 simulation units of time, which corresponds to a time period of 7.1 Gyr. The Plummer softening length is 40 pc for stars and 100 pc for dark matter. Energy conservation is achieved to 1% and angular momentum to 0.5% .

4. Results

Our simulation results can be enumerated as follows:

- strong warping of the outer parts of the disk ($r > 5$ scale lengths) sets in early; the warp is sustained to the end of the run (≈ 7 Gyr).
- strong flocculent spiral arms are noticed even near the edges of the disk where self-gravity is not strong enough to sustain such structure.
- MW disk develops a fast bar at about 3 Gyr though the M31 disk is found to be intransigent to bar formation. The pattern speed of the formed MW bar is found to decline from about $50 \text{ km s}^{-1} \text{ kpc}^{-1}$ to about $35 \text{ km s}^{-1} \text{ kpc}^{-1}$ by the end of the runs.

4.1. Warps

We quantify the strength of the warp that is triggered in the model disks, by analysing

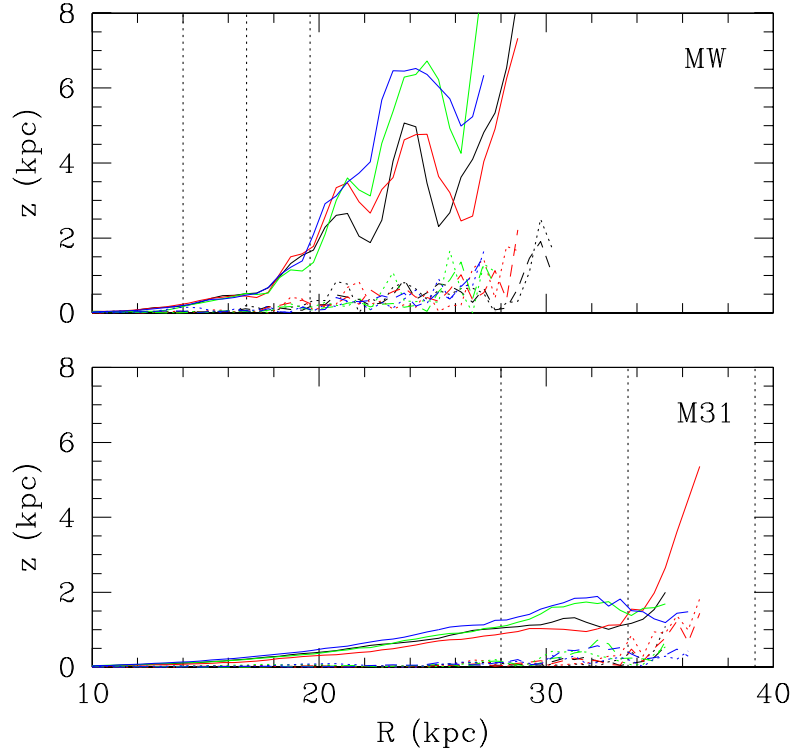


Fig. 1. Result of our warp quantification analysis for the model MW disk (upper panel) and M31 disk (lower panel). The quantification has been done in terms of the coefficients of the $m = 0$, (dotted lines), $m=1$, (solid lines) and $m = 2$, (dashed lines). The $m = 1$ warp is the strongest. Runs corresponding to different tumbling periods of 56, 28, 14 and 7 Gyr are shown in black, red, green and blue. The dashed vertical lines depict 5, 6 and 7 R_d .

the vertical deviation of disk particles from the midplane of the disk, across the radial range, using a Fourier expansion technique. This method quantifies the warp in terms of the coefficients of the m^{th} oscillatory terms. The result of the analysis for the MW and M31 models, quantified by the coefficients of the 0th, 1st and 2nd terms are shown in Fig. 1.

5. Discussion

The dynamical influence of the slowly rotating, triaxial, outer dark halo is studied in this

work. In particular, we address the effect that this has on the growth and sustenance of disk structures such as spiral pattern, bar and warp. While our MW model develops a bar at about 3 Gyr, the M31 model is robust to bar formation. Once formed, the bar instability is maintained till the end of the run (about 7 Gyr), though the pattern speed diminishes. Both model disks were noted to warp significantly, only in the outer parts (at radius in excess of about 5 R_d). Flocculent spiral arms were noted till the edge of the disks.

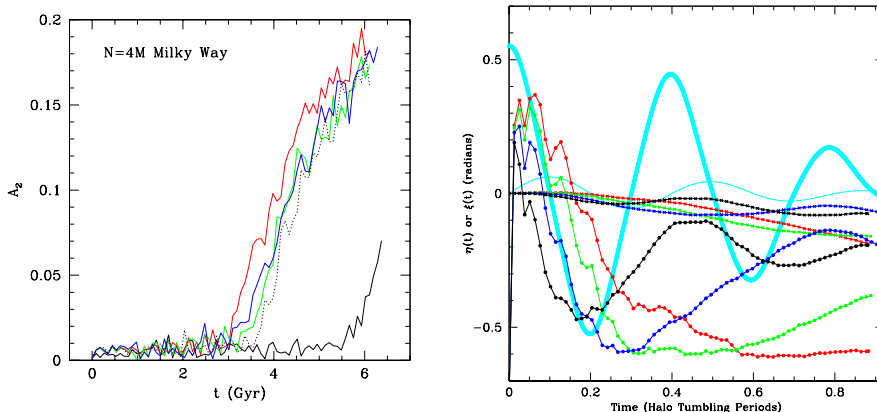


Fig. 2. Left panel: Evolution of the bar strength (A_2 parameter); the colour coding used here is the same as in Fig. 1, except that the lower isolated solid black curve denotes the growth of the bar in the control run. Right panel: η (thick cyan line) and ξ (thin cyan line) temporal oscillations, along the \hat{x} and \hat{y} axes respectively. The motion along these axes, from the runs done with the MW models are superimposed in different colours - red to black curves correspond to the slowest to the fastest moving halos. The η oscillations are in filled circles while the ξ oscillations are marked by crosses. The correspondence in the overall trend between the motion found numerically for the fastest halo and the analytically calculated motion is noted.

5.1. Analytical calculations

We realise that this problem is analytically tractable too, though the parameter realms within which we might have to stay confined will be constricted. We start by attempting to constrain the potential of a triaxial tumbling halo. If this is achieved, the equations of motion can be solved to give the orbits. This is indeed the basic idea behind the calculations.

The potential of triaxial systems have been discussed earlier (Binney & Tremaine 1987). Now, the lack of significant number of detections of non-circular velocities and oval distortions in the planes of high surface brightness disk galaxies indicates that on these planes, halos are nearly axisymmetric¹. Inspired by this, we choose to simplify our calculation by assuming axisymmetry in place of triaxiality - in fact, we perform our calculations in the oblate geometry. Also, we choose to work with a disk-halo misalignment of 90° , which is a larger misalignment than what is used in the simulations. The potential energy of the axisymmetric disk, in the field of the quadrupolar term in the halo potential turns out to have a bear-

ing on the various model parameters used, and importantly, bears unequal contributions from forces along two mutually orthogonal axes on the plane of the disk (say the \hat{x} and \hat{y} axes). This anisotropy is manifest through a dependence on the halo eccentricity as well as on the tumbling rate.

The equations of motion are solved, given this calculated potential energy. Under the assumptions of small halo flattening (eccentricity ≤ 0.4) and small deviations from the disk plane, the equations of motion are solved in a perturbative way. Precession and nutation are found to characterise these orbits - the precession period is calculated to be about 7.6 Gyr. The resulting orbits are of course dependent on the model parameters. The oscillatory motion along \hat{x} and \hat{y} , when compared to the evolution of the spin axes in the MW model, as found from our runs with the MW model, exhibit an overall similarity between the analyti-

¹ Of course, the situation may be different in dwarfs and low surface brightness systems which manifest much larger non-circularity (Valenzuela et al. 2007; Hayashi & Navarro 2006).

cally and numerically established motion (see right panel of Fig. 2).

The dynamical mechanism that we discuss in our work is noted to leave a significant imprint on the evolution of disk structures, in terms of the formation of the bar, warp and spiral pattern in the disk. We envisage further numerical investigation of this important mechanism.

References

- Bailin, J., Kawata, D., Gibson, B. K., et al. 2005, *ApJ*, 627, 17
- Bailin, J., & Steinmetz, M. 2004, *ApJ*, 616, 27
- Barnes, J., & Efstathiou, G. 1987, *ApJ*, 319, 575
- Berentzen, I., Shlosman, I., & Jogee, S. 2006, *ApJ*, 637, 582
- Binney, J. 2007, in *Island Universes, Structure and Evolution of Disk Galaxies*, ed. R. S. de Jong (Springer, Berlin), 67
- Binney, J., Jiang, I.-G., & Dutta, S. 1998, *MNRAS*, 297, 1237
- Binney, J., & Tremaine, S. 1987, *Galactic Dynamics* (Princeton Univ. Press, Princeton)
- Bureau, M., Freeman, K. C., Pfitzner, D. W., & Meurer, G. R. 1999, *AJ*, 118, 2158
- Dubinski, J. 1992, *ApJ*, 401, 441
- Dubinski, J. 1996, *New Astronomy*, 1, 133
- Dubinski, J., & Carlberg, R. G. 1991, *ApJ*, 378, 496
- Dubinski, J., & Kuijken, K. 1995, *ApJ*, 442, 492
- Franx, M., & de Zeeuw, T. 1992, *ApJ*, 392, L47
- Frenk, C. S., White, S. D. M., Davis, M., & Efstathiou, G. 1988, *ApJ*, 327, 507
- García-Ruiz, I., Kuijken, K., & Dubinski, J. 2002, *MNRAS*, 337, 459
- Hayashi, E., & Navarro, J. F. 2006, *MNRAS*, 373, 1117
- Jiang, I.-G., & Binney, J. 1999, *MNRAS*, 303, L7
- Jing, Y. P., & Suto, Y. 2002, *ApJ*, 574, 538
- Kalirai, J. S., Guhathakurta, P., Gilbert, K. M., et al. 2006, *ApJ*, 641, 268
- Kuijken, K. 1991, *ApJ*, 376, 467
- Kuijken, K., & Tremaine, S. 1994, *ApJ*, 421, 178
- Navarro, J. F., Frenk, C. S., & White, S. D. M. 1995, *MNRAS*, 275, 56
- Nelson, R. W., & Tremaine, S. 1995, *MNRAS*, 275, 897
- Sackett, P. D., Rix, H.-W., Jarvis, B. J., & Freeman, K. C. 1994, *ApJ*, 436, 629
- Sellwood, J. A. 2003, *ApJ*, 587, 638
- Shen, J., & Sellwood, J. A. 2006, *MNRAS*, 370, 2
- Sparke, L. S. 1984, *MNRAS*, 211, 911
- Sparke, L. S., & Casertano, S. 1988, *MNRAS*, 234, 873
- Spergel, D. N., Bean, R., Doré, O., et al. 2007, *ApJS*, 170, 377
- Toomre, A. 1983, in *Internal Kinematics and Dynamics of Galaxies*, IAU Symp. 100, ed. E. Athanassoula (Reidel, Dordrecht), 177
- Valenzuela, O., Rhee, G., Klypin, A., et al. 2007, *ApJ*, 657, 773
- van der Kruit, P. C. 2007, *A&A*, 466, 883
- Warren, M. S., Quinn, P. J., Salmon, J. K., & Zurek, W. H. 1992, *ApJ*, 399, 405
- Weinberg, M. D. 1998, *MNRAS*, 297, 101
- Weinberg, M. D., & Blitz, L. 2006, *ApJ*, 641, L33
- Widrow, L. M., & Dubinski, J. 2005, *ApJ*, 631, 838